FullControl GCode Designer: open-source software for unconstrained design in additive manufacturing

Andrew Gleadall

Wolfson School of Mechanical and Manufacturing Engineering, Loughborough University, Loughborough, Leicestershire, LE11 3TU, UK

E-mail: a.gleadall@lboro.ac.uk   Tel: +44 (0) 1509 227 578

AUTHOR VERSION

PUBLISHER VERSION AVAILABLE AT HTTPS://DOI.ORG/10.1016/J.ADDMA.2021.102109

Graphical abstract

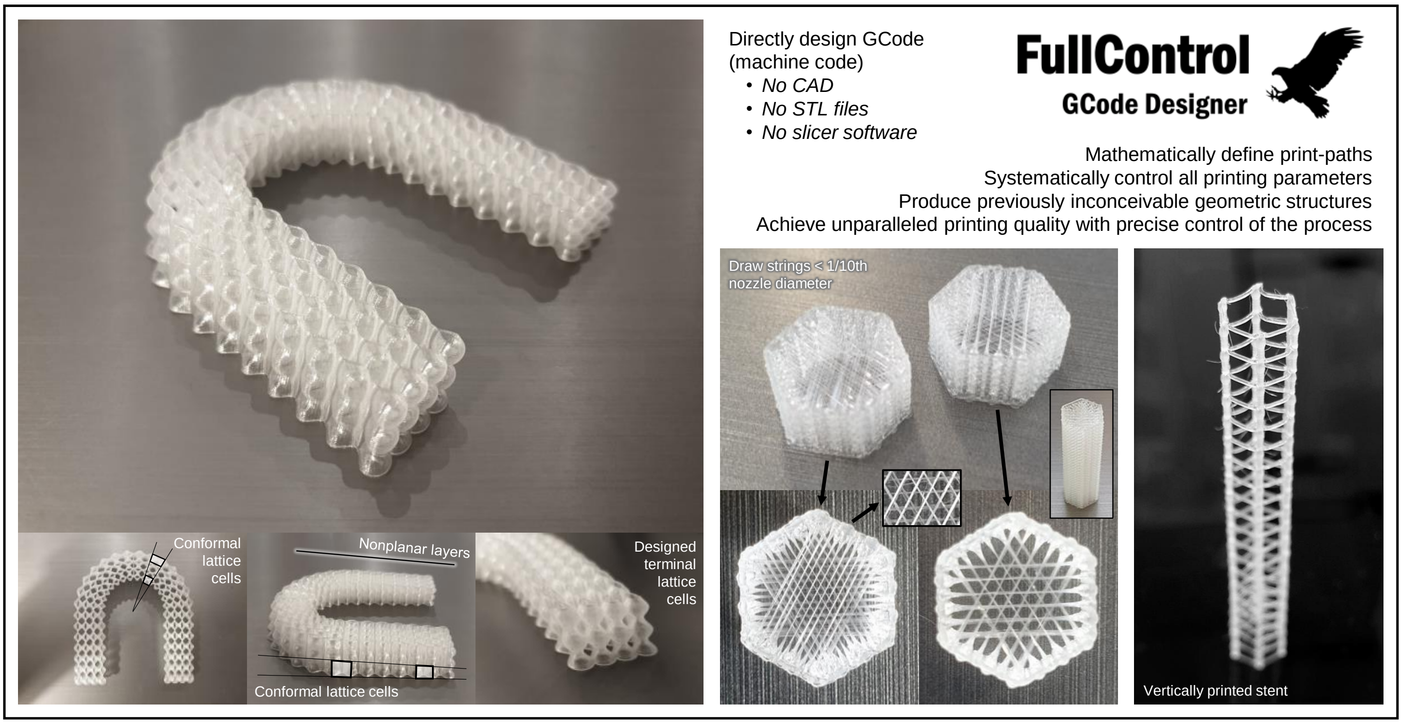

Abstract

A new concept is presented for the design of additive manufacturing procedures, which is implemented in open-source software called FullControl GCode Designer. In this new design approach, the user defines every segment of the print-path along with all printing parameters, which may be related to geometric and non-geometric factors, at all points along the print-path. Machine control code (GCode) is directly generated by the software, without the need for any programming skills and without using computer-aided design (CAD), STL-files or slicing software. Excel is used as the front end for the software, which is written in Visual Basic. Case studies are used to demonstrate the broad range of structures that can be designed using the software, including: precisely controlled specimens for printer calibration, parametric specimens for hardware characterisation utilising hundreds of unique parameter combinations, novel mathematically defined lattice structures, and previously inconceivable 3D geometries that are impossible for traditional slicing software to achieve. The FullControl design approach enables unconstrained freedom to create nonplanar 3D print-paths and break free from traditional restrictions of layerwise print-path planning. It also allows nozzle movements to be carefully designed - both during extrusion and while travelling between disconnected extrusion volumes - to overcome inherent limitations of the printing process or to improve capabilities for challenging materials. An industrial case study shows how explicit print-path design improved printer reliability, production time, and print quality for a production run of over 1,000 parts. FullControl GCode Designer offers a general framework for unconstrained design and is not limited to a particular type of structure or hardware; transferability to lasers and other manufacturing processes is discussed. Parametric design files use a few bytes or kilobytes of data to describe all details that are sent to the printer, which greatly improves shareability by eliminating any risk of errors being introduced during STL file conversion or due to different users having inconsistent slicer settings. Adjustable parameters allow GCode for revised designs to be produced instantly, instead of the laborious traditional routine using multiple software packages and file conversions. The FullControl design concept offers new opportunities for creative and high-precision use of additive manufacturing systems. It facilitates design for additive manufacturing (DfAM) at the smallest possible scale based on the fundamental nature of the process (i.e. assembly of individual extrusions). The software and source code are provided as supplementary data and ongoing updates to improve functionality and the user interface will be available at www.fullcontrolgcode.com.

Keywords

DfAM; Calibration; Toolpath; Manufacturing plan; Slicer software.

1. Introduction

In the last twenty years, material extrusion additive manufacturing (MEAM) has grown from a prototyping technology to one that produces intricate structures such as tissue engineering scaffolds [1–3], electronic components [4–6] and spatially designed fibre-reinforced components [7,8]. MEAM also has the ability to use materials that are difficult to process with other manufacturing technologies such as cell-laden hydrogels [3,9,10] and ceramics [11–13]. These materials and applications are generally associated with a shift in the use of MEAM technology towards higher value applications, where fidelity and defects are critical, as opposed to prototyping.

This shift is also evident from the development of new MEAM systems in recent years; for example, to allow continuous carbon fibre reinforcement (e.g. Markforged X7 and Anisoprint ProM IS 500) and metal printing (e.g. Desktop Metal Studio System; Markforged Metal X). For more intricate structures, more challenging materials and higher value applications, problems associated with the print-path, which is typically generated using 3D printing slicing software, are of more critical importance.

A recent review paper highlighted that *“suitable methodologies have yet to be established to fully enable and exploit the true potential of [functionally graded additive manufacturing]”* and identified a need for new approaches for print-path generation [14]. The limitations of slicing programs, and constraints they put on the user, have led to custom print-path scripts being developed for several research studies [15–17]. The need for new design software has also been identified industrially, as demonstrated by the following extract from an article by Sarat Babu, founder of the additive manufacturing company Betatype:

“One of the big challenges [for additive manufacturing design] is that software really needs to be informed by the entire process from design to production. On the design side, we need tools that help us to explore the design space, unconstrained” [18]

In contrast to design approaches that provide design freedom by excluding manufacturing considerations, this study presents a generic framework for users to explore the design space for structures that can only be achieved by coupling the designed geometry with the manufacturing procedure. This is important for parts in which geometric features are of a similar size to the process resolution or when the geometry is directly affected by process parameters.

Some relevant software has been developed to allow precise control for specific fields and applications, including: layerwise scaffold design for bioprinters [19], printing in well plates for bioprinters [20], graded scaffolds [21], fibre placement for carbon fibre reinforced printers [22–24], continuous extrusion for ceramics [11], controlled discontinuous extrusion for ceramics [13] and integration of multiple processes [25]. Additionally, scripts to translate CAD sketches or vector graphics into print-paths have been developed [26,27] as well as scripts for post-processing GCode generated by slicers [28]. However, the approach presented here is the first generic framework (i.e. it is not limited to a particular type of print-path or print procedure) developed for the unconstrained design of print-paths and associated printing parameters. Importantly, it allows the design of non-geometric GCode, to control manufacturing aspects beyond the geometric print-path. The software is described conceptually and practically in the next two sections. Case studies in Section 4 demonstrate its unique capabilities to achieve parts that would be difficult or impossible to achieve using other methods.

2. FullControl GCode Designer: concept description

The typical approach to generate GCode is a multi-step process (Figure 1A) involving CAD, STL file conversion and slicing software, which slices the model into layers and identifies a print-path for each layer, resulting in GCode (an example line of GCode shown in Figure 1B). Each step involves limitations and introduces errors [29].

In the FullControl design approach, a practical framework has been developed which allows the print-path to be explicitly defined (Figure 1A) along with all parameters for each individual segment of the print-path, including:

- Direction
- Print speed
- Extrusion rate (controlling extrudate height/width) or set as a non-extruding ‘travel’ movement
- Material choice (or print head/tool number)
- Other relevant parameters (e.g. acceleration/jerk, nozzle temperature, bed temperature, fan speed)

The user defines each step of the manufacturing plan in a sequential manner. This is similar to features being created and modified in a CAD feature tree. In contrast to CAD, the design information provided by the user fully defines the whole manufacturing procedure. The user designs a sequence of 3D lines, including all data in the bullet points above, with the potential to also include non-geometric GCode text strings at any point in the sequence. The practical implementation of this approach, described in Section 3, overcomes the complexity of defining potentially millions of X-Y-Z coordinates through functionality similar to linear and polar arrays in CAD packages or through mathematical definition (i.e. curve equations).

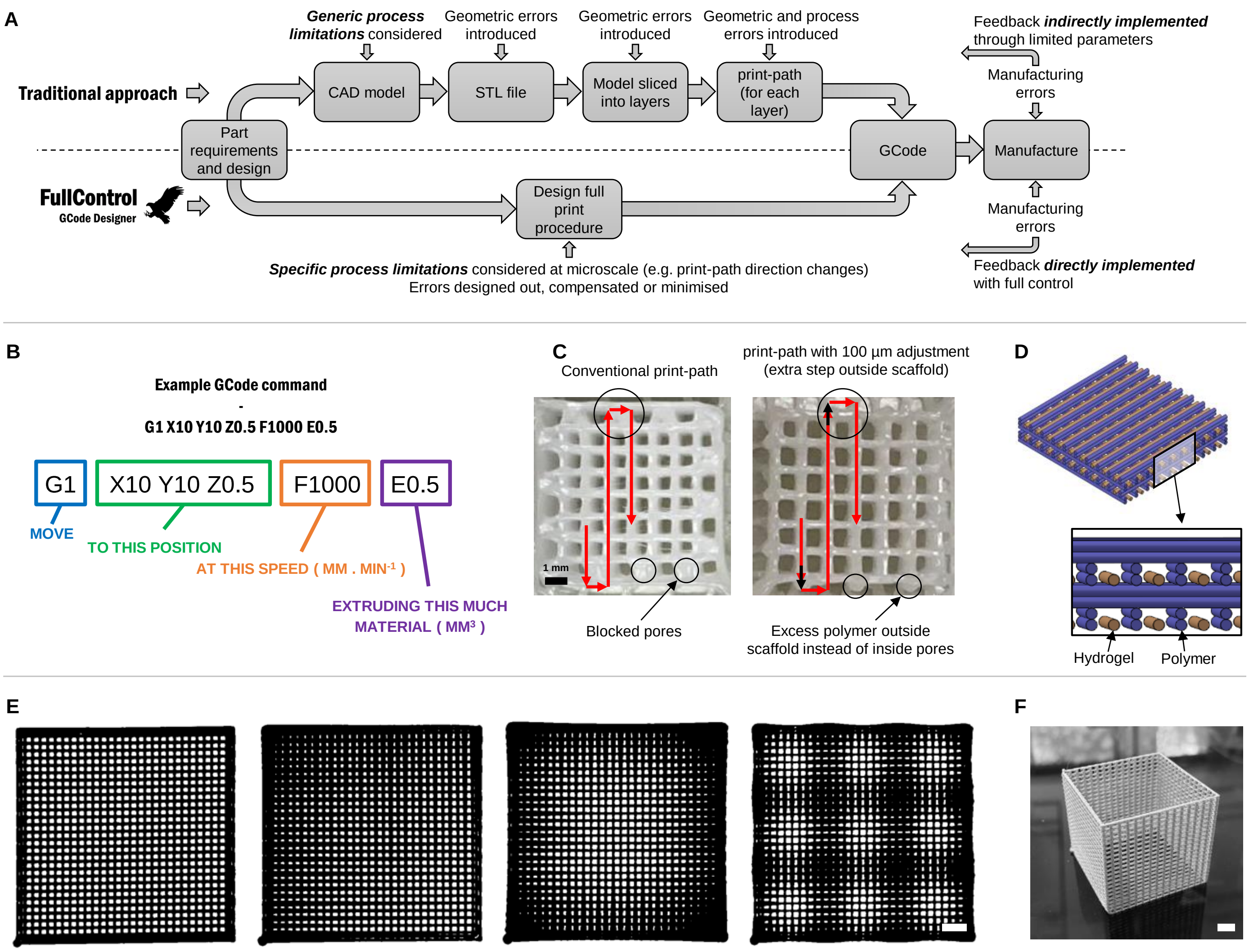

Figure 1 The FullControl design approach and example parts. A) Flow chart comparing the traditional approach using 3D printing slicing software and the FullControl approach, in which the geometric print-path and all non-geometric printing instructions are explicitly designed. B) Example line of GCode for one print-path segment. C) Example adjustment to the print-path (moving the nozzle outside of the structure) [30]. *D) Example print-path with multiple materials printed at different heights above the print platform in a designed non-sequential manner [3]. E) An identical print-path was used to print several different graded meshes, by designing a variable extrusion width* [31]. *F) A single-filament-wide mesh wall printed by combining vertical extrusion (away from the print platform) with horizontal extrusion (parallel to the print platform). All parts of the figure, even when linked to publications, were created from original media. Scale bars = 5 mm unless otherwise indicated.*

A tissue engineering scaffold structure from recent research [30] is used as an example to introduce the FullControl approach and potential benefits (Figure 1C). The typical approach to manufacture lattice scaffolds is to create a cuboid CAD file and select slicing software parameters to achieve a porous grid print-path. A commonly seen flaw in such structures is that uncontrolled extrusion blocks pores at the edges (Figure 1C). This can be caused by multiple factors, including: (i) acceleration and deceleration at the boundary of the structure, which allows more time for extrusion, (ii) the printhead moving along the boundary and therefore ‘double printing’ some segments of the grid, leading to wider or offset extrusion, and (iii) extruded material being dragged laterally by the nozzle after direction changes. When the toolpath was designed with the FullControl design approach, a minor adjustment overcame the issue of blocked pores by considering process limitations: the print-path was designed to deposit the undesired excess material away from critical regions. A small extension of the printed line that directly crosses the structure was designed (Figure 1C), which meant excess deposition occurred on the external surface (non-critical geometry) rather than inside pores (critical geometry). This simple adjustment was not possible using conventional 3D printing software, and too cumbersome to implement in bioprinting software. It is important to optimise processes to minimise the source of errors; for example, by using 'linear advance' algorithms to achieve consistent extrusion at corners or instantaneously stop extrusion to prevent 'double printing'. But in some cases, such optimisation may be challenging (e.g. specific firmware; Bowden printers; flexible materials). Therefore, process optimisation and process-informed design should be combined in a complementary manner.

In addition to overcoming process limitations, explicit print-path design provides opportunities to break free from the traditional approach of printing layers sequentially, as shown in Figure 1D. Several layers of polymer were printed before printing hydrogel at a lower height within a recess, to (i) allow the less viscous hydrogel to be contained within the polycaprolactone scaffold, and (ii) to ensure the hydrogel did not flow onto the top surface of the polymer, which would have interfered with interlayer bonding.

The FullControl design approach also enables freedom beyond geometric print-path design. Extrusion rate and speed were continuously varied in a recent study [31] to achieve five different graded lattice geometries for an identical print-path (Figure 1E). In the FullControl design approach, it is also possible to parametrically vary retraction, temperature, acceleration and any other parameter that can be controlled with GCode. The GCode is generated in the same format as that produced by slicers and it is possible including advanced firmware algorithms and associated settings for compatible printers (e.g. by inserting an "M900 K0.18" command to adjust 'linear advance' settings).

2.1. Key advantages

The distinguishing capability of FullControl GCode Designer, and its underlying design approach, is unconstrained freedom for users to design every aspect of the printing procedure. It empowers users to design structures in a completely new way and enables a wide range of technical additive manufacturing operations that are challenging or impossible for slicing software, as shown by case studies in Section 4. It allows intricate consideration of process limitations and for the control of auxiliary equipment. New software (described in Section 3) is required for the approach to be practically achievable: manual editing in a text-based GCode editor would be too complicated and time consuming for all but the simplest of structures. One-off GCode-generation scripts, CNC machining software, and software for converting CAD geometry into GCode are all focused on specific types of geometry or manufacturing procedures, and do not allow for generic design of wide-ranging additive manufacturing procedures.

Many benefits of the FullControl design approach originate from it instilling a completely different way of thinking about design and from it changing the overall workflow for GCode creation:

- A new way of thinking for design
    - X, Y and Z coordinates, as well as extrusion volume, speed and other settings are simultaneously considered for each segment of the print-path. This facilitates unconventional print-paths and print settings; for example, in nonplanar print-path design, extrusion rate can be designed to vary with layer height.
    - Non-extruding travel movement is fully designed. Therefore, associated defects can be eliminated or minimised, including the position of stringing, undesired deposition, nozzle collisions with lips at part edges, top-surface scoring from fast-travel nozzle movement, and shear deformation of structures as the nozzle moves away from them.

- Custom GCode strings are a natural part of the design process since they are defined at the same time as the print-path. Therefore, any aspect of the process that is controllable with GCode can be implemented in the design. For example, pauses can be designed to allow stabilisation and focus of a microscope tool.
    - Mathematical definition of print-paths is possible in combination with non-mathematical geometry, which allows complicated print-paths to be simply and parametrically defined.
    - Feature-based design of GCode means each print-path segment or GCode instruction can be modified after initial creation. This allows for intricate control of specific points in a manufacturing procedure and enables parametric calibration procedures to be designed.
    - Simplicity of the print-path is naturally encouraged to minimise design effort. Although this limits part-shape complexity (discussed in the next section), simple print-paths reduce the scope for unanticipated errors. Each unnecessary step in a printing procedure, such as retraction or fast travel movement, introduces additional risk of failure (e.g. material feed issues or part detachment from the print platform). Therefore, designing simple continuous print-paths with smooth nozzle movement and no retraction improves printing reliability.
- Benefits of the new workflow and software
    - No programming skills are required to generate the GCode.
    - Parametric feature-based design means file-size efficiency is high and GCode can be parametrically adjusted without reproducing a CAD model, STL file and slicing procedure.
    - The full manufacturing plan is designed from start to finish, and it can be directly translated between printers without the risk of inconsistencies due to different users' slicer setups.
    - No data transfer errors are introduced due to the elimination of conventional conversion processes from CAD to STL to sliced layers to print-paths.

2.2. Key limitations

One limitation is that a reasonably high level of process expertise is required to design a print-path and set all print parameters. The user must be aware of factors that are often set automatically in slicing software, such as cooling fan speed, priming the nozzle before printing, and understanding the challenges involved in stopping extrusion and travelling (without extrusion). However, with appropriate guidance from an expert, even novice users can achieve high-quality results quickly. For example, the mesh structure in Figure 1F was technically designed and manufactured by a project student (see Acknowledgements) within two weeks of first using a 3D printer. This sort of structure (a porous single-filament-wide wall) had never been produced before due to the lack of software accommodating the FullControl design approach, but may have broad potential applications, including filters, biomedical meshes, vascular models and fluid flow devices. It demonstrates that this limitation (i.e. the need for process expertise) can be negated if an expert guides the user to only vary parameters that are relevant to their application, for example by providing a pre-created design file. Ways to reduce requirements for process expertise are being investigated, including the creation of design templates and integration of the design approach into existing slicing software.

A second limitation is that complicated non-systematic print-paths are technically challenging for human design. Many typical components would be difficult to design using the presented method due to discrete changes in geometry requiring different print-paths in different locations. The design effort may still be justified if print reliability or quality is critical. The risk of human error must also be considered when the designer is given more control. A key strength of slicing software is the ability to undertake millions of computations (identifying print-path coordinates) that would be unfeasible for a human. For typical components to be designed using the presented approach in an accessible manner, some of the automation aspects of slicing software would need to be incorporated into the print-path design process. The distinction between well-suited and poorly suited geometry is not obvious, but in general, the FullControl approach is most suited to structures where coordinates can be identified systematically or mathematically.

A final consideration is that some hardware systems use a proprietary machine control code format, as opposed to a GCode text file, or use web-based software that cannot be loaded with custom-written GCode. These systems are currently unsuitable for FullControl GCode Designer without direct collaboration with the hardware developer. For systems that require an unusual format of GCode, a simple revision to the GCode formatting algorithm would be required.

3. FullControl GCode Designer: practical implementation

Akin to how CAD packages provide a framework for the generation of 3D models, FullControl GCode Designer provides a framework for the generation of print-paths. Additionally, whereas CAD offers the user the capability to assign details such as material or tolerance requirements to each part of the model, FullControl offers the user the capability to assign printing details such as print speed and print direction to each part of the printing procedure.

The practical implementation presented here for the FullControl design approach allows the user to sequentially describe every segment of the print-path by defining 'features' in an Excel spreadsheet, line by line, including details about how the printer should operate as it traverses each individual segment. FullControl interprets the list of features in the sequence in which they were defined by the user, similar to a feature tree in CAD: the GCode described for the first feature is generated before the next feature is evaluated, which may generate new GCode, or adjust or replicate GCode that was generated by earlier features.

As with CAD, the user defines 'features' using a range of feature-types, which are shown in Figure 2 and described in this section. The most fundamental feature-type is to define a 'print-path segment' (Section 3.1). A second fundamental feature-type is to define a 'custom GCode string' (Section 3.2). Additional feature-types (Section 3.3) improve usability - for example, to allow print-path segments to be repeated in a linear or polar array. The actual software implementation of FullControl GCode Designer is described in Section 3.4, including an example design workflow. Availability of the software is described in Section 3.5.

3.1. Fundamental feature-type 1: print-path segment

For each print-path segment (i.e. G0 or G1 command in GCode), the user defines:

- Coordinates of the start of the segment (mm)
    - X, Y, Z values - directly equivalent to the coordinate system used by the printer and GCode
    - Alternatively, polar coordinates may be used (automatically converted to Cartesian in GCode)
- Coordinates of the end of the segment (mm)
- Information about the amount of extrusion during the print-head movement for this segment
    - Option 1: define the nominal width and height of the filament (mm)
    - Option 2: explicitly define the magnitude of 'E' in the GCode - typically identifying the length of feedstock-filament to feed into the printer for this print-path segment (mm)
    - Option 3: select 'travel' motion, in which no extrusion occurs, and speed is typically fast
- Speed of the print head whilst printing the segment ($mm.min^{-1}$)
- Print-head ID (for multi-material or multi-tool printers)

Additional parameters for specific systems could be incorporated in revised versions of FullControl (by modifying the open-source code), including pressure for pneumatic syringe systems, or equivalent aspects for other extrusion system designs and alternative manufacturing tools.

3.2. Fundamental feature-type 2: custom GCode string

As opposed to creating a line of GCode that instructs the printer to move the print head, the 'custom GCode string' feature-type allows the user to give non-geometric instructions to the printer by inserting a GCode string during the printing process. This is useful for aspects such as:

- Retraction
- Temperature (nozzle, print platform, chamber)
- Acceleration and jerk
- Fan speeds
- Homing axes
- Pausing the print for inspection or insertion of prefabricated components
- Outputting information to the display screen
- Adding comment lines to GCode to improve human legibility
- Controlling auxiliary equipment such as cameras or ultraviolet curing lights

To allow for parametric variation, the custom GCode string can be defined as a concatenation of multiple strings and numbers, as opposed to a single text string. This enables the numeric values to be adjusted each time the line of GCode is repeated - as recently used to incrementally increase acceleration in a single test print, allowing the identification of which acceleration values caused greatest fluctuations in extrusion due to resonant vibration (often called 'ringing') [31].

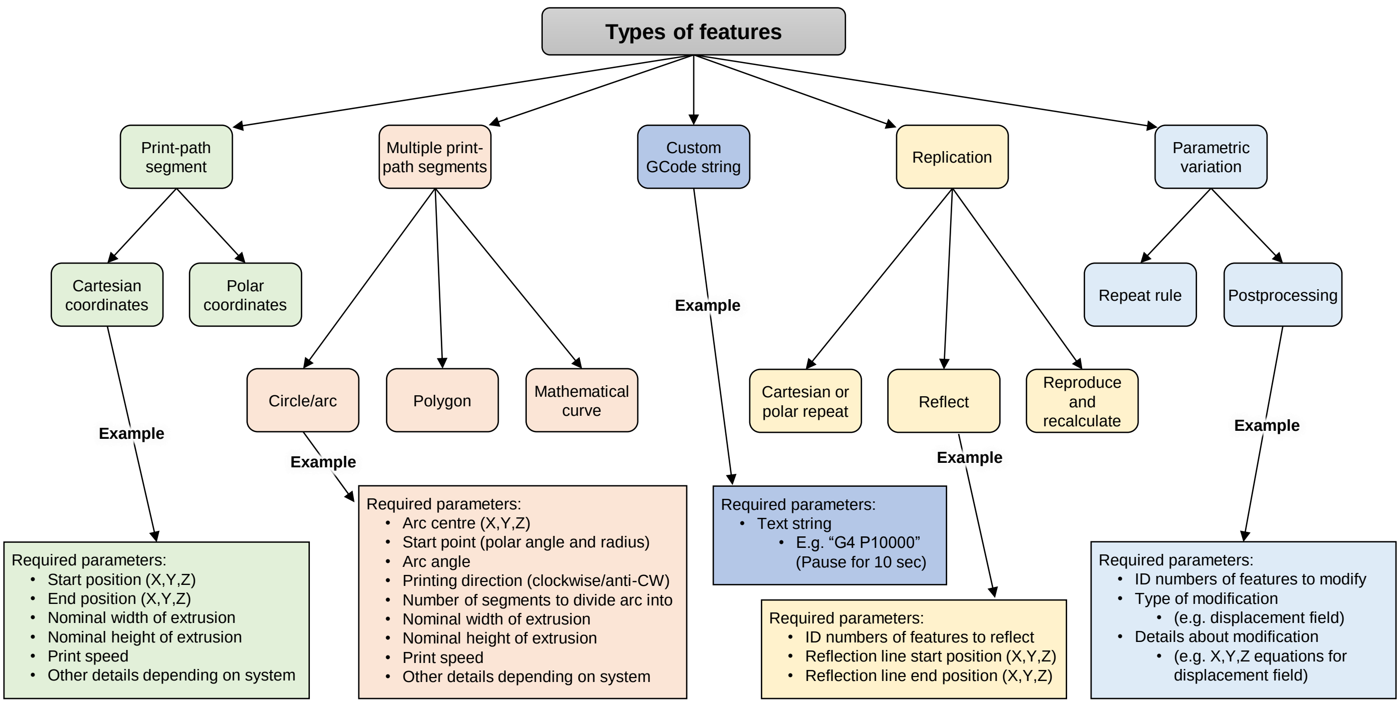

Figure 2 *Map of the different feature-types that are provided in FullControl GCode Designer to design a print-path and/or associated non-geometric instructions. Examples indicate which parameters must be defined by the user for five feature-types. Features are created sequentially and evaluated by the software in a similar manner to a CAD feature tree.*

3.3. Additional feature-types for practical design

Additional feature-types allow the user to design complicated structures without needing to manually define the coordinates of every print-path segment, which would be unfeasible for structures with thousands of segments. Instead, the user describes the desired print-path in a manner that allows FullControl to identify the coordinates. It is important to state that FullControl does not make any decisions: all aspects are fully defined by the user and FullControl is simply undertaking the associated numerical calculations. Full details are given here for the circle/arc feature-type as an example (also discussed later in relation to Figure 3B), whilst other feature-types are briefly described (detailed information for all feature-types is included in the software). Three main categories of the additional feature-types (besides those in Sections 3.1 and 3.2) are:

- Multi-segment geometry
    - Circle/arc - for an arc in an X-Y plane, the user describes the arc geometry and all necessary information for FullControl to automatically determine the individual print-path segments (as opposed to manually defining them), including:
        - X-Y-Z values of the arc-centre
        - Polar angle and radius of the start point
        - Arc angle (360° = circle)
        - Direction of printing (clockwise or anti-clockwise)
        - Number of segments (the arc is printed as a series of straight segments)
        - Information about extrusion amount, speed and print-head ID (as required for manual definition of a print-path segment in Section 3.1, unless inherited from overall settings)
    - Polygon – the user defines polygon size, shape, orientation and order/direction to print the sides.
    - Mathematical curve - user defines X/Y/Z or polar equations for nozzle movement, which allows printing of sinusoidal waves, spirals, or any other mathematical curve. Speed and extrusion rate may also be varied according to a mathematic equation.
- Replication of existing features
    - Cartesian and polar repeats - the user identifies which previously defined features should be repeated and gives geometric details for the repetition. A critical distinction from CAD is that, in addition to replicating print-path segments, replication feature-types also replicate non-geometric GCode (e.g. retraction). This is important because if a single layer is designed and then repeated multiple times using a cartesian array feature, it is essential that all GCode instructions are repeated, not just the segment coordinates. This highlights a key distinction between FullControl GCode Designer and scripts that translate CAD drawings to GCode.
    - Reflection - to create mirror images of previously defined features, for print-paths with reflective symmetry.
    - Reproduction and recalculation of mathematical equations - for equations that are functions of the current nozzle coordinates (e.g. its current position above the print bed), it is necessary to recalculate the associated print-path segments each time the equation feature is repeated.
- Parametric variation rules
    - ‘Repeat rule’ - this rule allows aspects of the print-path or parameters to be varied in a systematic manner. For features that have been replicated multiple times (e.g. replicating an identical print-path for multiple layers), the user can describe how the print-path or parameters vary for a specific replicate-range or to incrementally vary with each repetition. As an example, a single-filament-thick micro-tensile-testing specimen was recently developed, in which dog-

bone geometry was achieved by incrementally varying extrusion width for each printed layer (see discussion related to Figure 4A for more details).

  - ‘Postprocessing’ - this feature-type also allows user-selected previously defined features to be modified. It is similar to the ‘Repeat rule’ feature-type but can be applied to all features as opposed to only those that are created during a replication feature. In many cases, the same design can be described using either a ‘Repeat rule’ or a ‘Postprocessing’ feature, but the distinction may be advantageous for more complicated designs.

The above feature-types are demonstrated in the next section and in case studies.

3.4. Software overview and design workflow

To embed the sequential nature of GCode into the design process, features are defined in the order in which they are ultimately written in the GCode file. Each new feature (and the necessary parameters for its definition) is entered by the user in a new line in the user interface in FullControl GCode Designer. Microsoft Excel was chosen as the user interface due to its ability to facilitate parametric and mathematical definitions and its widespread availability and use. Since the FullControl design approach is based around explicit definition of numerical values, Excel is naturally well suited to it and enhances design capabilities in a way that typical user-input forms would constrain. The FullControl framework’s program code is written in Visual Basic (approximately 2,500 lines of code). Once the user has defined all the features in their design, the GCode is generated and can be previewed in the user’s preferred software (e.g. Repetier Host [32]).

An auxetic lattice is used to exemplify several feature-types of FullControl and demonstrate the design workflow, which involves the following steps:

1. Conceptually design the part geometry
    - Typically, hand-drawn sketches - see leftmost schematic in Figure 3A
2. Design the overall print-path sequence
    - Typically, hand-drawn schematics on gridline paper - see central layer-by-layer schematics in Figure 3A
3. Identify geometric information necessary to fully define the print-path
    - Typically, annotations on the print-path schematic, such as arc-centre coordinates in absolute or relative terms - see rightmost schematic in Figure 3A. Similar to how engineering drawings contain all necessary information to allow a part to be manufactured in a workshop, these annotated print-path schematics contain all necessary information to allow the part to be created in FullControl. For mathematical feature definitions, graphing calculators are useful to develop equations [33].
4. Design the print-path in FullControl - see Figure 3B, which is explained in the paragraph following these bullet points
    - Use coordinate data already identified in the schematics discussed above. There are infinite different ways to create an identical print-path, similar to how a sphere could be modelled in CAD using many different functions (e.g. filleting a cylinder or cube, or revolving a semicircle)
5. Preview the print-path during the design process and before manufacture - see Figure 3C-H
    - The print-path preview supports iterative development of bullet points 1-4

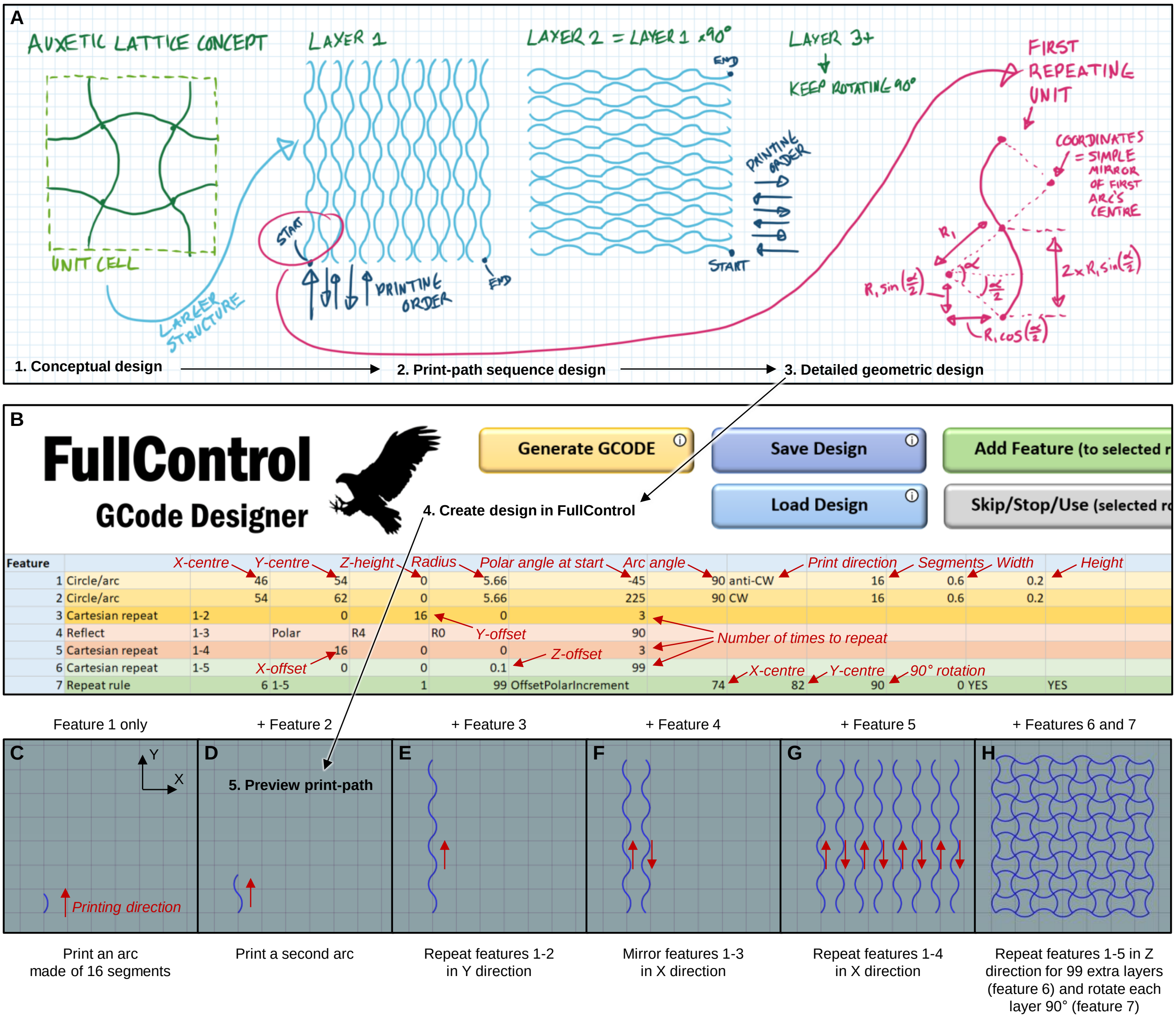

Figure 3 *Design workflow for the FullControl design approach. A) Hand-drawn schematics are useful to (1) conceptually design the structure, (2) design the print-path sequence to achieve the concept structure, and (3) identify the detailed geometric information necessary for technical design of the structure in the FullControl software. B) User interface screenshot of FullControl GCode Designer, showing seven features that describe the design in (A) and are evaluated sequentially to generate GCode. Parameters of the 'Circle/arc' feature are identified with labelled arrows for cross-reference to Section 3.3. C-H) Previews of the GCode after sequential inclusion of each of the seven features in (B). The arrow-linked steps labelled 1 to 5 are listed and described in Section 3.4. Grid in (C-H) = 10 mm.*

The FullControl user interface with the completed design for the auxetic lattice example is shown in Figure 3B (provided as the 'Lattice' example design in the software [34]). Print-path previews are shown after each feature was created (Figure 3C-H), to demonstrate the continuous and systematic nature of the design method. These previews also show how the features are aggregated and sequentially evaluated by the software. Features 1 and 2 in Figure 3B both generate new GCode for arcs. Features 3-6 are all evaluated to replicate the GCode commands of previous features with modified coordinates (Cartesian offset or reflection). Feature 7 is evaluated to modify the coordinates of the GCode generated in feature 6: to rotate the position of print-path segments in each layer by 90° in the X-Y plane. The parameters for the first feature Figure 3B (a circle/arc feature) are identified with labelled arrows for cross-referencing to the description of the circle/arc feature-type in Section 3.3. Particularly relevant parameters for other features are also identified to support interpretation of the respective print-path preview images on 10-mm grids. The most complicated aspect of this design is the trigonometric calculation of arc centre points and rotation points for each layer - highlighting the importance of detailed schematics (rightmost image in Figure 3A). Other features were created with ease. The design was created to be entirely parametric (unit cell size, number of unit cells, arc curvature, number of layers, layer height and filament width). This simple design resulted in over 100,000 lines of GCode, which took just 14 seconds to generate. When the design parameters are saved as a comma-separated values (csv) file, they require 300 bytes, with lossless quality. This is in the region of four orders of magnitude smaller file size than an STL file, which would have geometric errors and not contain any information about print-path, direction, speed and similar aspects. These benefits of parametric design have led to dedicated software to define the 3D geometry of lattices, such as nTopology [35]. In addition to allowing designs with adjustable parameters, conditional statements can easily be incorporated in a design - for example, features may be activated for certain conditions, such as switching from three to four perimeters if a parameter for part size exceeds a threshold value.

FullControl also incorporates some necessary functionality that is not associated with the design of the printed structure. In particular, the instructions at the start and end of the GCode file are specific to a given printer and ensure it begins printing correctly and finishes the printing process safely (e.g. disabling heaters). Therefore start-GCode and end-GCode instructions are incorporated into all generated GCode files. Before using FullControl for a new printer, the start-GCode and end-GCode must be identified from the user manual of the printer or by examination of existing GCode.

Other functionality has been included in FullControl to improve the usability, such as saving/loading designs, disabling/enabling features, creating adjustable parameters, describing coordinates in absolute or relative manners (i.e. relative to the nozzle position at the end of the previous feature), and the addition of automatic travel movements if the user creates disconnected print-path segments (e.g. between the first and second printed waves in Figure 3F). However, it is recommended as good practice to explicitly define all print-path segments, including non-extruding travel segments. Additionally, there is a section in the software user interface where information about the overall printing process is entered, such as default printing speeds and temperatures.

Video S1 (<2 min) in supporting data [34] highlights some of the structures enabled by FullControl and includes video clips of the 3D printing process. Video S2 (≈20 min) in supporting data [34] gives a detailed technical introduction to FullControl with live-recorded demonstrations of features being defined and GCode being generated.

The software has evolved over several years, iteratively improving to allow increasingly complex structures, as shown in the case studies in Section 4. This has led to practical software, which has been extensively tested for over a thousand hours by more than twenty students and researchers and used for several thousand hours of printing on systems ranging from £200 to £200,000.

3.5. Software availability and development

FullControl GCode Designer is open source and permanently available in a research data repository [34]. It is being further developed, and updated versions of the software will be available from www.fullcontrolgcode.com. Specific developments or new functionality may be requested by contacting the author of this article.

4. Demonstrations and discussion

This section demonstrates the FullControl design approach with a series of case studies. All manufactured parts were designed and manufactured using FullControl GCode Designer or developmental versions of it. CAD software was not used (not even to support the design phase, despite the author and other software users being regular CAD-users) since schematics are naturally more appropriate and useful for parametric definition of designs, as discussed in the previous section.

Multiple printers were used (Ultimaker 2+, Raise3D Pro2, regenHU 3DDiscovery, German RepRap X400) but all structures are achievable with a wide range of materials using any MEAM system that reads GCode. It has been successfully used to print silicone, conductive inks and clay. The designs for case studies are included in the software [34] or described in associated journal papers.

4.1. Process calibration, characterisation and hardware development

It is common for GCode to be manually written for simple process calibrations - for example, to move the nozzle to set locations of the print platform to level it. FullControl allows the creation of such print-paths and much more complicated parametric calibration with little effort. FullControl GCode Designer has been used to calibrate or characterise:

- Print platform height/level - by printing multiple concentric squares
- Retraction settings - by printing a parametric array of discontinuous lines, with each non-extruding travel movement assigned a different amount of material retraction and retraction speed
- Fibre orientation in short-fibre-reinforced polymer
- Extrusion widths for different print settings
- Quality of different overhang angles
- Capabilities for entirely novel structures - as discussed later in relation to Figure 7
- Position of auxiliary hardware - by printing lines at controlled positions on the print platform

By allowing the design of non-geometric factors as well as the precise print-path, expansive parametric process characterisation procedures can be designed. A recent study characterised how the width of extruded filaments could be varied continuously along their length to achieve a new scale of design for MEAM (discussed later in relation to Figure 4D) [31]. That study investigated hundreds of different combinations of speed, acceleration, jerk, retraction, extrusion width, and other parameters. By enabling design geometric tolerances an order of magnitude smaller than the nozzle diameter,, a new micro-tensile-testing specimen was designed with extrusion-widths of filaments carefully controlled to achieve a dog-bone geometry (Figure 4A) [36,37]. This demonstrates the potential to design at completely new scales if process limitations are considered. These tensile-testing specimens allowed higher throughput and more detailed characterisation of mechanical properties compared to sliced CAD models of ASTM specimens. The FullControl design for the specimens consisted of just seven features - it is provided as the 'TensileTestingBox' example design in the software [34]. FullControl readily allows direct comparison of different 3D printers because a single design can be used to generate identical print-paths and print parameters in multiple GCode formats. The micro-tensile-testing specimens have achieved comparable results by at least ten users, on twenty different printers, from five different system manufacturers, by avoiding any potential introduction of errors due to inconsistent slicer settings or similar.

Custom-developed hardware, such as printing on a mandrel or with a multi-process print head (e.g. utilising both material-extrusion and machining tools), is well-suited to the FullControl design approach due to the flexibility to design non-extruding tool movements and custom GCode strings.

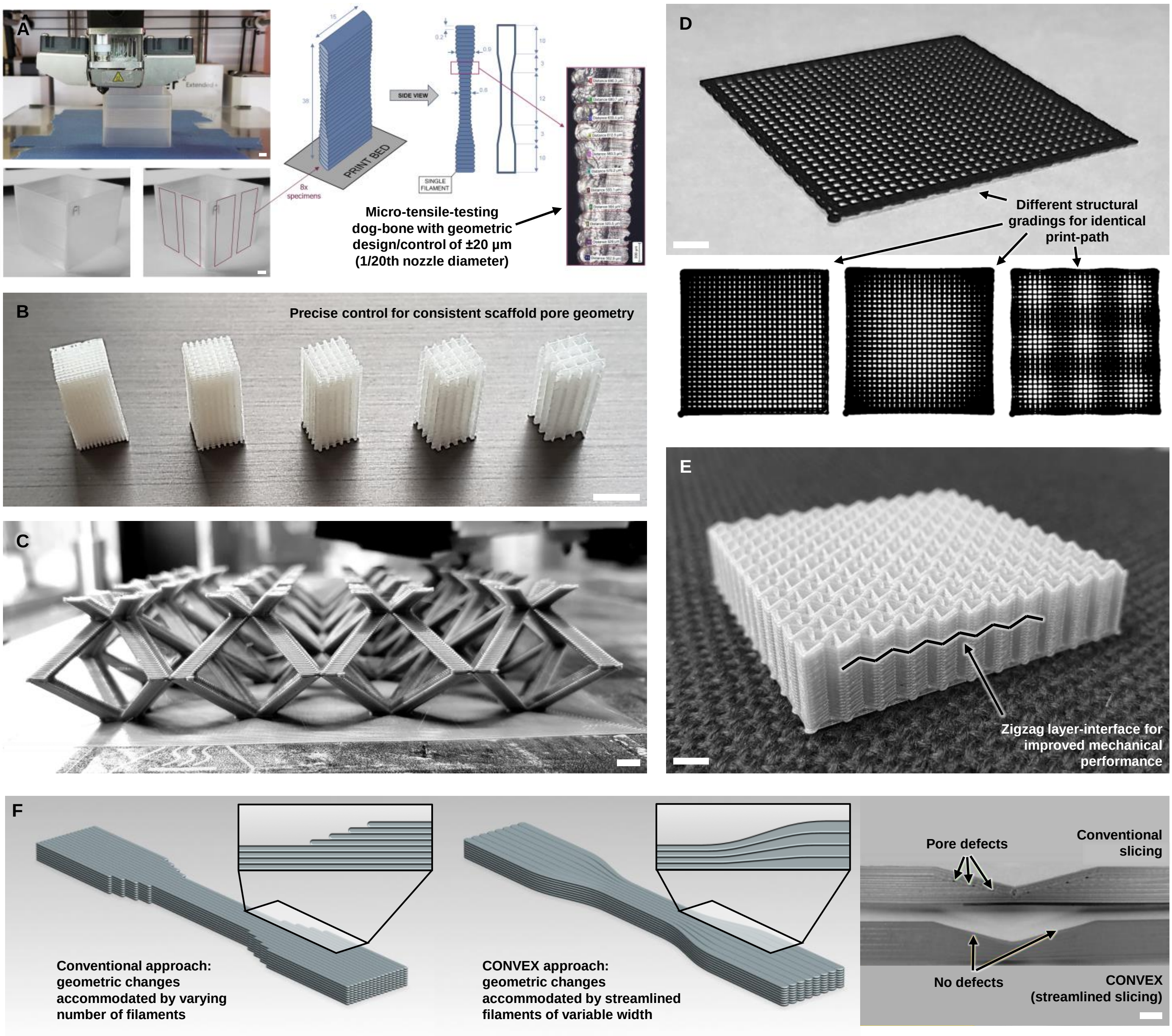

***Figure 4** Structures designed at the scale of individual filaments using FullControl GCode Designer. A) Micro-tensile-testing specimen with individually designed filament-widths. B) Tissue engineering scaffolds with different spacing between extruded filaments* [30]*. C) A parametric lattice structure, where each individual extruded filament was explicitly designed for a relatively large part (8 cm wide). D) Mesh structures produced with an identical print-path but variable extrusion-width, achieved by sinusoidal variation of print speed and extrusion rate* [31]*. E) Nonplanar printing using a zigzag print-path with up-down nozzle movement in the Z direction, normal to the print platform, to improve mechanical performance* [38]*. F) Streamlined extruded-filaments with continuously varying extrusion width to fit the overall part geometry* [31]*. Videos S1 and S3 in supporting data* [34] *show the printing process for (E) and (D), respectively. A) Reproduced under the terms and conditions of the Creative Commons CC BY-NC-ND 4.0 License* [39]*. All other parts of the figure, even when linked to publications, were created from original media. Scale bars = 5 mm.*

4.2. Filament-scale design and novel print-paths

For structures where the geometry of individual extruded filaments is critical, such as the micro-tensile-tensing dog-bone specimens in the previous section), explicit design of the print-path and print settings and settings for individual filaments is a logical approach. This also applies for structures where the pores between individual filaments are critical (e.g. tissue engineering scaffolds in Figure 1C) or where individual extrusion of different material are assembled (e.g. printed electronics or scaffolds in Figure 1D). However, the lattice structure with six-filament-wide struts in Figure 4C demonstrates the benefits of the FullControl design approach for larger structures, to allow explicit definition of:

i. the order in which struts were printed
ii. the exact order and direction in which each filament was printed for each strut
iii. the manner of travel between struts, which involved multi-step movements of the print head to ensure excess extrusion was deposited in the centre of struts rather than their external surface
iv. parametric geometry, which allowed the print-path to be instantly regenerated for new parametric designs

The microscale control enabled by the FullControl approach allows the geometry of individual filaments to be designed along their length, as opposed to considering filaments to have an unvarying geometry. This allows entirely new structures to be conceived, such as the graded mesh materials in Figure 4D; even though an identical print-path was used for all structures, geometric grading was achieved by sinusoidal variation of print speed and extrusion width [31]. This highlights how unconstrained design of the printing procedure enables new conceptual printing approaches. Although the geometry of individual filaments must be designed, adding a level of complexity, this can be a simple design process when using parametric or mathematic functions such as sinusoidal fluctuation. Mathematic design is discussed further in Section 4.3. The FullControl approach is appropriate for larger assemblies of extruded filaments, as demonstrated by it use to uninhibitedly investigate a new conceptual slicing strategy, 'streamlined slicing' [31], in which streamlines of the part geometry were used to define the print-path, and extrusion width was continuously varied based on the separation of these streamlines (Figure 4F). In this case, the ability to control acceleration independently for each print-path segment was important, highlighting the benefit of parametric design of both the print-path and print parameters.

A key opportunity enabled by the FullControl design approach is the unconstrained ability to design print-paths utilising all three dimensions, as opposed to the conventional approach of completing X-Y movements (print-platform plane) before moving by one layer-height in the Z direction (normal to the print platform). This allowed research into mechanical performance enhancement by using nonplanar interfaces between layers (Figure 4E): zigzag interfaces disrupted the fracture path and led to improved mechanical performance versus conventional planar layers [38]. The most important aspect to note here is not the improved performance, but rather that FullControl enabled investigations that were not possible with existing software. There is an infinite range of other structures and aspects that could be investigated. Controlled print-path design in the Z direction is further utilised in several examples in subsequent sections (discussions related to Figure 5D&E and Figure 7).

4.3. Mathematical design

When designing print-paths with FullControl GCode Designer, a useful approach is to define the paths with mathematical functions. Several examples of this are shown in Figure 5 and discussed here. The sinusoidal cylinders in Figure 5A were all produced with the same parametric design, with slightly adjusted parameters. In FullControl, the design consists of just one feature - a mathematically defined spiral curve with sinusoidal fluctuation of radius. The equations for X, Y and Z coordinates can be seen in the 'SineTube' example given in the software [34]. This simple design format allows the full detail of the design to be recorded with a few bytes of data, whilst allowing parametric generation of GCode with thousands or millions of print-path segments.

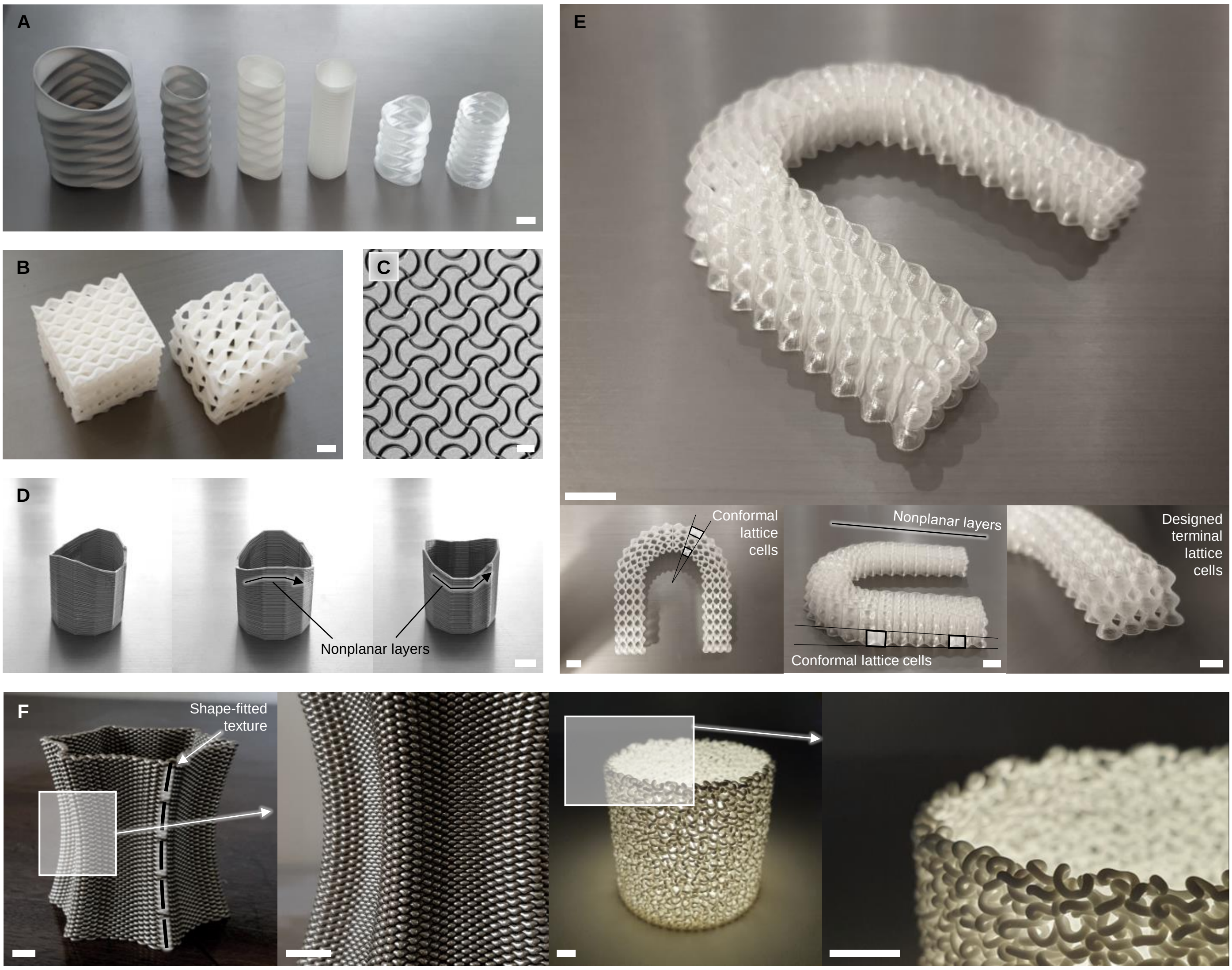

***Figure 5** Mathematically defined structures produced using FullControl GCode Designer. A) Parametric spiral print-path with sinusoidal fluctuation, created with a single design feature in FullControl. B) Gyroid lattice structures. C) Lattice structure considered in Figure 3. D) Dodecagonal cylinder with sinusoidally varying layer height designed with just three features in FullControl. E) A concept shoe sole with conformal lattice geometry, nonplanar layers and specially designed terminal lattice cells - designed with just thirteen features in FullControl. F) Mathematically defined textures. Videos S1 and S4 in supporting data* [34] *show the printing process for (C) and the manufactured part in (E), respectively. Scale bars = 5 mm.*

Mathematically defined lattices are also well-suited to FullControl because the curve equations for the print-paths on each layer can be readily determined from theoretical mathematical descriptions of the lattices. The gyroid structures shown in Figure 5B required just 15 features in FullControl. This design allowed full parametric variation of unit cell sizes, the number of unit cells, and many other design or printing parameters. Over 500,000 lines of GCode were produced, depending on the structure size, and the computation time is less than two minutes (with scope for significant software-code optimisation for computation speed). In this ongoing research, the ability to control every print-path segment on every layer allowed investigative freedom and design optimisation for additive manufacturing that was not possible when using CAD and slicer software.

The printed version of the structure in Figure 3 is shown in Figure 5C, which used trigonometric definitions for design parameters. Additionally, the potential to vary layer height according to a sinusoidal function is shown in Figure 5D for a dodecagonal cylinder, which had the same number of layers along the entire circumference; this allowed the nonplanar top-surface of the part to be printed in a single pass, eliminating stepping that traditionally occurs between printed layers. The design is included as the 'NonplanarCylinder' example in the software [34].

A mathematically defined concept shoe sole is shown in Figure 5E. The print-path for one layer was defined mathematically, including considerations to conform the lattice to the part geometry (top-down view in bottom-left image). Conforming the lattice resulted in immense improvement in part quality compared to what would be achieved by filling an STL file (of the overall part geometry) with a regular lattice, which would have partial cells. Partial cells were also avoided by designing the terminal unit cells to have a different structure, enabling a neat external surface (bottom-right image in Figure 5E). This highlights a key capability of the FullControl framework to combine mathematical curve equations with non-mathematical features such as arcs or 'cartesian repeat' features. By fully designing the print-path, it was possible to avoid non-extruding travel movements (a common cause of defects, especially for flexible polymers such as polyurethane used here). The ability to modify the print-path on different layers (using 'repeat rule' features) allowed non-vertical walls (skewed inwards) to be designed whilst maintaining a conformal lattice and avoiding any partial unit cells. The ability to design freely in all three dimensions allowed the straight side-sections to be printed with nonplanar layers to achieve varying part thickness whilst avoiding stepping artefacts associated with layerwise manufacturing of shallow gradients. Again, the design approach naturally allowed a conformal lattice for the nonplanar layer geometry (middle-bottom image in Figure 5E). Creating a CAD model of this part would be extremely inefficient and challenging, and would result in a poor product quality since errors would be introduced by the STL file conversion and by the generation of a print-path that would almost certainly include non-extruding travel movements. By comparison, a fully parametric design was created in FullControl (approximately 1 kilobyte of data versus an estimated 1 gigabyte for a non-parametric STL model) using just thirteen features: five mathematically defined lines, three features for repetition or reflection of those lines, and five features to define geometric skew and nonplanar modifications. These features resulted in 210,000 lines of GCode.

As well as overall part geometry, mathematical definition of the print-path allows for the design of microscale features, as shown for textured parts in Figure 5F. A parametric design was created in which the print-path fluctuated sinusoidally to achieve a rippled texture. The magnitude and frequency of fluctuation is adjustable with user-defined parameters, along with other aspects of the design including overall size, shape, layer height and extrusion rate. To achieve the structure to the right in Figure 5F, parameters for layer height and extrusion rate were increased, as described in the design file, which is provided as supplementary information [34], including example parameter sets. The design is usable without any understanding of the mathematical print-path formulae, highlighting how expert knowledge can be integrated into a print-path design for team projects and collaboration. Since Excel is used as a front end for FullControl, it was possible to include usage instructions in the design file, along with parameter descriptions and a customised user interface with images of print-paths for example parameter sets.

4.4. Industrial manufacturing

In response to a short-term need for face visors, a suite of twenty 3D printers were used to manufacture over 1,000 reusable visor-frames (Figure 6A). This case study has high industrial relevance due to the high production-volume, relatively large part dimensions, considerable time constraints, and specific customer requirements. The parts were sent for post-processing and assembly by Toyota Motor Manufacturing UK, who in turn liaised with healthcare end users. Some key constraints and considerations were:

- Nylon material had to be used (to ensure reusability), which can be challenging to retract.

- Bowden-tube printers had to be used; these present an additional challenge for retraction due to the longer distance between the extruder and nozzle compared with direct-drive printers
- Only minor revisions to the geometric design were permitted
- Significant time constraints limited the potential for optimisation compared to typical research work
- The printing procedure had to be resilient for reliable manufacturing on twenty printers, which often behaved considerably differently

After manufacturing, the parts were post-processed to remove defects such as protrusions or strings, especially on the forehead band and in the visor slot. Post-processing was the bottleneck of the overall production process, so reducing post-processing time was a key aspect of optimisation.

Despite several days of refinement by multiple experienced users with two different slicing software packages, the printing speed was limited by defects associated with the print-path and non-extruding travel movements of the nozzle between sections of the part (see string-defects in Figure 6C). By fully defining the print-path using FullControl, it was possible to minimise the number of non-extruding travel movements and ensure they occurred in non-critical areas. This is shown in Figure 6F, which compares previews of the slicer-generated GCode that was originally being used to the final FullControl GCode. In particular, non-extruding travel movements were avoided for the forehead band (in contact with the user's forehead) and the slot into which the visor sheet fitted. The successful reduction of stringing can be clearly seen in Figure 6C. Stringing was particularly prominent because the speed and extrusion width were set as high as they could be before introducing under-extrusion defects. Retraction capabilities were limited due to requirements for a high material flow rate, Bowden fed printers, and nylon material. For other situations, slicing software may be much more successful, but here, it was invaluable to be able to control the position of defects and undesired strings to be located in accessible areas (e.g. visor bolt holes which were rapidly post-processed with a hand drill). In addition, where possible, the print-path was designed to perform retraction and un-retraction operations in internal regions to minimise surface blemishes.

Originally, a large proportion of post-processing effort went into ensuring that the forehead band was smooth. With FullControl, the band required no post-processing because it was printed with a single pass of the nozzle, extruding 250% of the nozzle diameter (aspect ratio of 5 for width:layer-height). This was found to achieve a solid structure with good mechanical integrity, as expected based on recent understanding that a wider aspect ratio for filament cross-sections improves mechanical performance [37] (discussed in Section 4.1). Due to improved mechanical integrity, it was possible to reduce weight by 20% whilst maintaining equivalent or improved performance. This highlights the potential to integrate expertise of process limitations into the design of the print-path (and relevant printing parameters) to improve performance.

Printing speed was also improved by designing a smooth continuous print-path. No infill was used, and the part was printed using large sweeping arc motions. The smooth nature of the print-path improved aesthetic quality (eliminated defects/blemishes), and dramatically reduced the mechanical stresses put on the printers (when the nozzle quickly changes direction hundreds of times to complete infill of narrow regions).

To allow multiple parts to be printed overnight without supervision, it was desirable to print a stack of visor bands in a single printing procedure (Figure 6A). Under-extrusion was deliberately employed to achieve discontinuous droplets of extruded material. This can be seen in Figure 6D, which shows three still images of the printing process at two-second intervals; the inset image to the right shows a zoomed-in view of a single under-extruded line made up of connected droplets. This type of discontinuous deposition provided sufficient support to achieve good quality for subsequent parts, whilst also allowing part-separation by hand.

Towards the end of the printing process, the part geometry required material to be printed in between the front and rear walls of the visor slot (to connect these two regions). Printing perpendicularly across this slot is the conventional approach to bridging it. However, this would have resulted in a staggered print-path and eliminated many of the benefits of the smooth sweeping print-path design described above. Therefore, a sinusoidally fluctuating arc was printed for one layer, to bridge the slot and act as support for slot-aligned print-paths in subsequent layers. This is shown in Figure 6E, where the left two images show the sinusoidal bridge during and after printing, and the right image shows it after two lines have been printed on top of it (aligned with the slot) on the subsequent layer. The mathematical definition of the sinusoidal bridging line made it far simpler to implement in FullControl than to define numerous perpendicular bridging lines, highlighting the practical potential to incorporate mathematical design (as discussed in Section 4.3) for mundane and functional purposes.

The following benefits of parts produced using FullControl GCode Designer (instead of slicing software) are direct quotations from a senior manager at Toyota Motor Manufacturing UK (Daniel Nelson):

1. *"Increased product output from both printer speed increase and stacking on the print bed*
2. *Reduced post-production time due the improved quality including surface finish*
3. *Raw material reduction through weight optimisation*
4. *Printer reliability improvement as the machines ran smoother"*

Overall, the production rate increased by 400% to 600% per printer, whilst also significantly reducing the time-demands on the printing technician, due to a combination of stacking, reduced weight, and increased printing speed. An improved product was achieved in terms of the business customer (Toyota - especially in terms of post-processing time) and the end user (in terms of comfort on the forehead).

Although this section directly compares the FullControl approach to slicers, it should be considered as a demonstration of potential applicability of the new design approach rather than an evaluation of slicing software. The print-path preview in Figure 6F indicates a reasonably typical slicer print-path, but it could be improved using advanced capabilities of slicing software such as custom print settings in different regions of the model. Some aspects of the FullControl print preview appear leaner than the slicer version in the figure, but this mostly is due to the graphical representation: the extrusion width of the FullControl version was 250% of that for the slicer version, which is not apparent in the preview lines. Also, the attachment point for the elastic headband was oriented vertically instead of horizontally, so it was printed on every layer of the FullControl print-path, as opposed to only on some layers in the slicer version. Overall, the attachment-points were similar in size for both designs. This is a good example of the design process encouraging the simplest possible print-path. Rather than using support structures and conventional design rules such as 45° overhangs to achieve horizontal attachment points, the design requirements were met by a simple print-path design. An almost identical print-path was used on every layer, except some print-path segments in top/bottom regions were replaced with non-extruding travel movements to allow a gap between the visor frame and the attachment point, into which the elastic headband slotted. This allowed top and bottom layers to be identical, to facilitate neat vertical stacking of visors.

The visor demonstrates the use of the presented design method beyond academic research, but it is a relatively simple geometry. Many 3D printed components, especially those manufactured by polymer printing systems with small nozzles and complicated print-paths, would be impractical for explicit print-path design. For the FullControl approach to be successful, it is important to consider the print-path early in the design process. The improvements to the printing procedure explained in this section would not have been possible if using scripts for GCode generation - too many different scripts would have been required (multiple print-path concepts were tested). Repeatedly rewriting scripts for small changes to the printing procedure would have overly burdened progress and have been infeasible given the time constraints. The design was described by 125 features in FullControl and took 4 minutes to generate 700,000 lines of GCode for a stack of eight visor-frames. It is provided as supplementary information [34].

For reasonable production runs (e.g. several hundred units), the effort/cost required for print-path design is justified by the benefits in terms of product quality, raw-material usage, printer maintenance, wastage for failed/rejected parts, production time and post-processing time. Print reliability is critically important for large structures, high-cost materials, materials with limited availability (e.g. autologous-cell-laden hydrogels), critical applications (e.g. medical implants), and many other fields. Therefore, improvements to print reliability may justify many weeks of effort to optimise the print-path design.

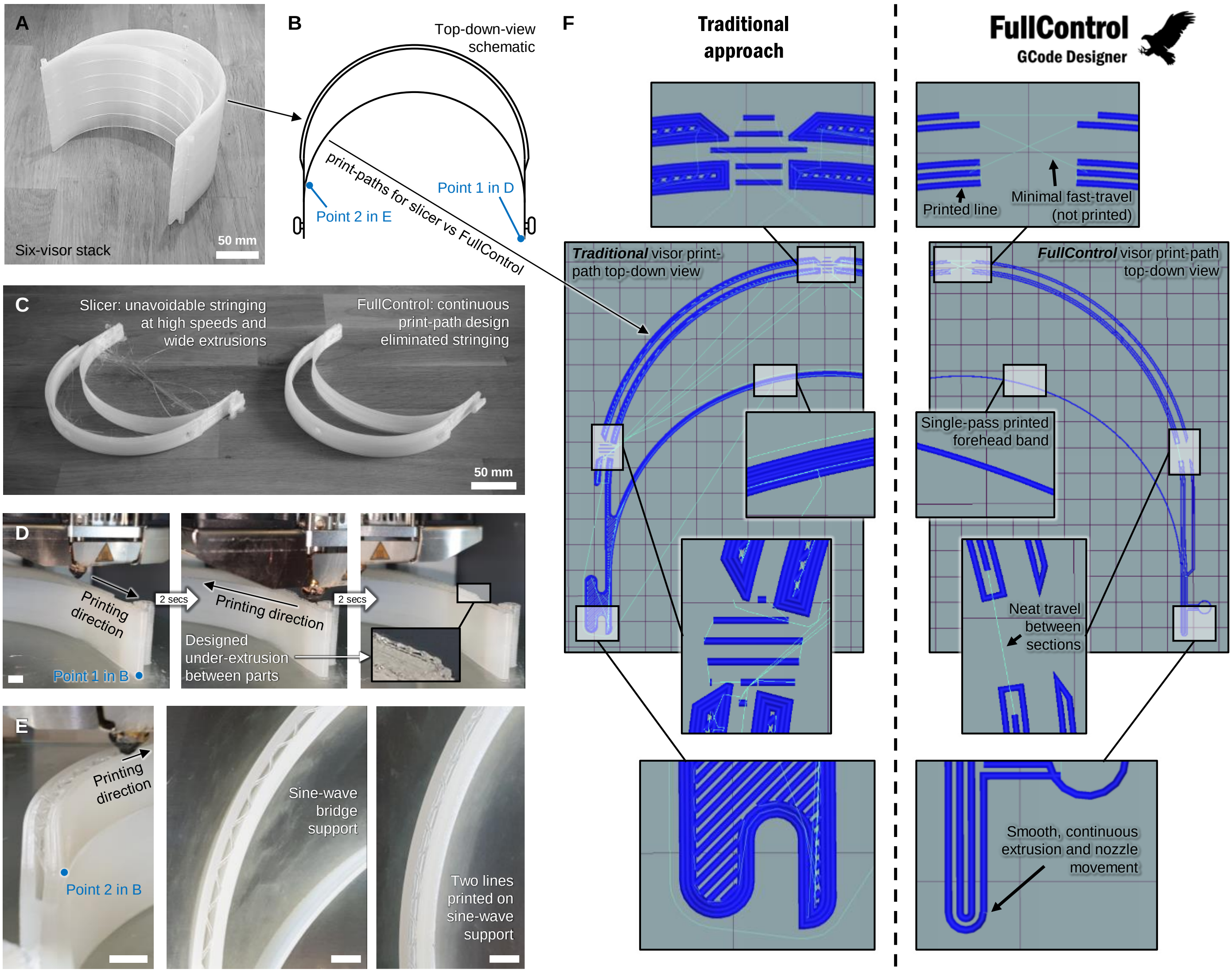

Figure 6 *Comparison between traditional slicer software and FullControl print -paths for a visor frame that was printed over 1,000 times. A) Stack of six visor frames printed together. B) Simplified top-view schematic of the print-path. C) Slicing software led to stringing and blemishes when printing at higher speeds. D) FullControl allowed precise design of under-extrusion between parts in a stacked print, resulting in connected droplets that sufficiently supported subsequent parts, whilst allowing separation by hand. E) A sine wave was printed to act as support when a gap needed to be bridged. F) Print-path previews for the original GCode produced by slicing software and the GCode produced by FullControl. By using the FullControl design approach, production rate increased by 400% to 600%, post-processing time was reduced, material usage was reduced, aesthetics was improved, comfort for the end-user was improved and printer reliability was improved. Video S5 in supporting data* [34] *shows the printing process for (E). Grid in (F) = 10 mm. Scale bars = 5 mm unless otherwise indicated.*

4.5. Novel structures

By having full control over both the print-path (with full three-dimensional freedom) and all additional relevant factors (e.g. extrusion rate and speed), it is possible to achieve entirely new geometric structures. An interesting structure is the normally undesirable strings that result from quick movement of the nozzle between different parts of the printed object. By carefully controlling vertical movement (normal to the print platform) along with extrusion rate and speed, it was possible to achieve a designed pattern of strings, as shown in Figure 7A, in which the nozzle was quickly moved between opposing sides of a pre-printed frame. This structure was used to calibrate the printing procedure to be able to control repeatability and geometric properties of the drawn strings. With FullControl, the addition of one simple feature ('Repeat rule' in Section 3.3) allowed each string to be printed with incrementally increasing speed, extrusion amount, vertical offset, and many other parameters. This allowed for rapid and informative characterisation of process capabilities for this previously unstudied structure. A variation of this calibration specimen was conversely used to optimise retraction settings to avoid strings when they were undesirable in other work. The design of a structure similar to that in Figure 7A is demonstrated in Video S2 in supporting data [34].

A more complicated implementation of strings, into a parametric hexagonal scaffold structure, is shown in Figure 7B. It was possible to achieve a precisely controlled structure with string diameters as low as 1/10th of the nozzle diameter, and repeatability such that 750 strings were all successfully printed in a single structure. These structures were designed with eight simply defined features in FullControl, and it took 1 second to generate 4,000 lines of GCode. Due to the ability to quickly iterate the structural design and generate GCode, the process of design and manufacturing optimisation for this highly unusual structure was completed in three hours. A CAD file cannot be created for these structures that has any meaningful data to allow their production using slicing software: they are only possible through explicit design of the GCode.

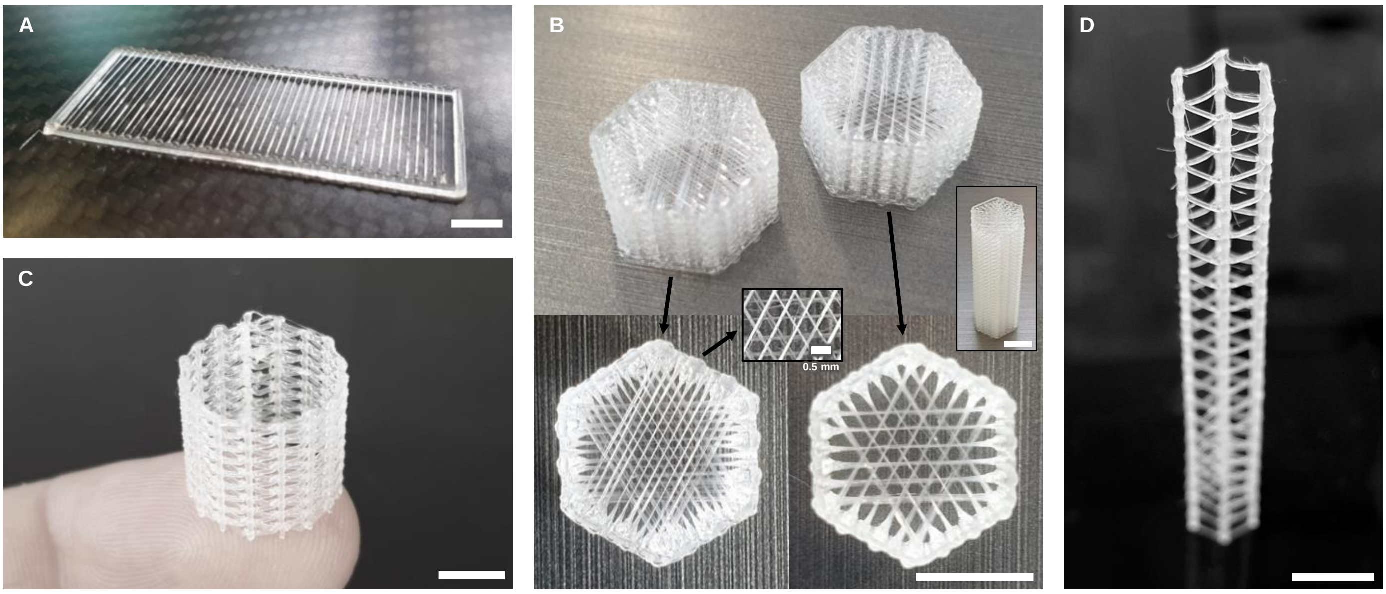

Figure 7 Novel structures produced with FullControl GCode Designer. A) Calibration specimen to optimise process parameters to manufacture repeatable drawn strings when the nozzle rapidly traverses from one side of a pre-printed frame to the other. B) Scaffolds manufactured by drawing strings across a hexagonal frame, with diameters as low as 1/10th of the nozzle diameter. 750 strings were printed in a taller variant (inset) with 100% success rate and high fidelity. C and D) Polylactide stent structures printed upright (central axis normal to print bed) using designed combinations of vertical extrusion (nozzle moving directly away from the print platform) and lateral extrusions. When crimped after manufacture, the stent in (D) self-expanded at elevated temperature. Video S1 in supporting data [34] shows the printing process for (B) and (C), and Video S2 demonstrates the design of (A). Scale bars = 5 mm unless otherwise indicated.

The ability to explicitly design speed, extrusion rate, and the 3D print-path are enabled the two demonstration stents in Figure 7C and D to be produced, which were printed vertically (central axis normal to the print platform). These structures were manufactured by using a combination of vertical extrusion of discrete pillars (moving the nozzle directly away from the print platform), followed by extrusion of bridging filaments between the pillars. This combination of extrusion-types was then repeated incrementally at increasing heights above the print platform to achieve several-centimetre-tall stents. These structures were only possible through careful parametric optimisation of the printing procedure, including the necessary design of multiple non-extruding 3D print-path segments to move the nozzle between pillars without deflecting them (or compromising their quality in other ways). The ability to design custom GCode strings for controllable pauses ensured a good connection between struts was achieved. The stent in Figure 7D was naturally self-expanding: it was crimped to less than half its initial diameter before naturally expanding to the original diameter at elevated temperatures. These structures break free from typical perceived constraints of printing layer-by-layer; slicing software is conceptually and practically incompatible with their design and manufacture. By designing printing procedures without constraints of typical software, entirely new applications for material extrusion additive manufacturing are possible.

4.6. Alternative processes

Whilst the described case studies considered the material extrusion additive manufacturing process, there are many other process technologies that use GCode with a similar or identical format, which could benefit from FullControl GCode Designer, with minor or no modifications. Minor edits to the open-source code would allow considerable different GCode languages. A particularly relevant use of FullControl, for which research is ongoing, is to design laser paths for processes including:

- Laser cutting
- Laser surface modification
- Vat photopolymerisation
- Selective laser sintering and melting (SLS and SLM)
- Laser measurement devices

Aside from lasers, there are many other potential uses of GCode for positional control in manufacturing and other fields, where the FullControl design approach may be of value, including:

- Material jetting
- Directed energy deposition
- 3D welding
- Coordinate measurement machines (CMM)
- Computer numerical control (CNC) machining
- Motorised XY linear stages for any application

The potential of FullControl to parametrically vary the tool path and other parameters, such as speed, opens up the potential for rigorous fundamental research and final-product manufacturing.

5. Concluding remarks

Open-source software called FullControl GCode Designer was explained conceptually and in terms of its practical implementation. The typical workflow for directly designing GCode was described, and case studies highlighted the wide range of potential uses, from calibration prints for research studies to industrial collaboration for production runs >1,000. Advantages over existing additive manufacturing software were discussed. The direct design of GCode allowed structures that are inconceivable when using traditional software and offers greater potential for refinement of additive manufacturing procedures.

The design approach represents an alternative way of thinking about additive manufacturing, in which the individual print-path segments are deliberately designed along with all printing parameters for each segment (e.g. speed, acceleration, extrusion rate, temperature) to allow absolute control over the manufacturing process.

The generally accepted use of slicing software - and the lack of process-specific information incorporated in CAD files - has limited research progress by not allowing the fundamentals of the process (individual extrudates) to be effectively studied. This is evidenced by FullControl immediately enabling multiple recent publications (featured in case studies) that challenge the status quo. For parametrically defined geometries, it is achievable to define all details of the print-path. Typical 3D components, however, with non-systematic geometry, would be challenging to define the print-path for in many cases. The strength of slicing software is in its ability to handle any geometry and for rapid generation of acceptable, but not fully controllable, print-paths. Custom-scripts for one-off structures also overcome limitations of slicing software, but they are naturally limited to a single application and require programming, unlike FullControl.

The FullControl design approach offers the unconstrained ability to design print-paths and deliberately control any printing parameter for all sections of that print-path. Furthermore, it encourages innovation and creativity; particular opportunities are nonplanar printing, extrusion of material in nonconventional geometries, optimisation of print-paths for maximal quality/reliability, rigorous process characterisation, precise experimentation for computer model validation, and elimination of uncontrolled defects.

The author is keen to collaboratively support improvement of the software to be more capable and more usable; by adding simulation capabilities or integration into slicing software, for example.

Acknowledgments

Thanks to all the people who have used FullControl GCode Designer for their research; in most case studies, the resulting journal paper is referenced, but additionally, thanks to Leung YinMing for specimens in Figure 1F and Figure 7C/D, and John-Jo Pye for specimens in Figure 5B. Also, thanks to Vadim Silberschmidt for advice on this publication, and to Celal Soyarslan, Mary Lack, David Comberton and Simone Fontana, who were the motivation for parts in Fig. 4C, Fig. 5C, Fig. 5E and Fig. 5F, respectively.

References

[1] I. Zein, D.W. Hutmacher, K.C. Tan, S.H. Teoh, Fused deposition modeling of novel scaffold architectures for tissue engineering applications, Biomaterials. 23 (2002) 1169–1185.

[2] T. Serra, J.A. Planell, M. Navarro, High-resolution PLA-based composite scaffolds via 3-D printing technology, Acta Biomater. 9 (2013) 5521–5530.

[3] L. Ruiz-Cantu, A. Gleadall, C. Faris, J. Segal, K. Shakesheff, J. Yang, Multi-material 3D bioprinting of porous constructs for cartilage regeneration, Mater. Sci. Eng. C. 109 (2020) 110578.

[4] F. Daniel, J. Peyrefitte, A.D. Radadia, Towards a completely 3D printed hot wire anemometer, Sensors Actuators A Phys. 309 (2020) 111963. https://doi.org/https://doi.org/10.1016/j.sna.2020.111963.

[5] J.O. Hardin, C.A. Grabowski, M. Lucas, M.F. Durstock, J.D. Berrigan, All-printed multilayer high voltage capacitors with integrated processing feedback, Addit. Manuf. 27 (2019) 327–333. https://doi.org/https://doi.org/10.1016/j.addma.2019.02.011.

[6] S. Aslanzadeh, H. Saghlatoon, M.M. Honari, R. Mirzavand, C. Montemagno, P. Mousavi, Investigation on electrical and mechanical properties of 3D printed nylon 6 for RF/microwave electronics applications, Addit. Manuf. 21 (2018) 69–75. https://doi.org/https://doi.org/10.1016/j.addma.2018.02.016.

[7] A.N. Dickson, D.P. Dowling, Enhancing the bearing strength of woven carbon fibre thermoplastic composites through additive manufacturing, Compos. Struct. 212 (2019) 381–388. https://doi.org/https://doi.org/10.1016/j.compstruct.2019.01.050.

[8] H. Mei, Z. Ali, I. Ali, L. Cheng, Tailoring strength and modulus by 3D printing different continuous fibers and filled structures into composites, Adv. Compos. Hybrid Mater. 2 (2019) 312–319.

[9] K.A. Deo, K.A. Singh, C.W. Peak, D.L. Alge, A.K. Gaharwar, Bioprinting 101: design, fabrication, and evaluation of cell-laden 3D bioprinted scaffolds, Tissue Eng. Part A. 26 (2020) 318–338.

[10] S. Ji, E. Almeida, M. Guvendiren, 3D bioprinting of complex channels within cell-laden hydrogels, Acta Biomater. 95 (2019) 214–224.

[11] J. Hergel, K. Hinz, S. Lefebvre, B. Thomaszewski, Extrusion-based ceramics printing with strictly-continuous deposition, ACM Trans. Graph. 38 (2019) 1–11.

[12] T. Yu, Z. Zhang, Q. Liu, R. Kuliiev, N. Orlovskaya, D. Wu, Extrusion-based additive manufacturing of yttria-partially-stabilized zirconia ceramics, Ceram. Int. 46 (2020) 5020–5027. https://doi.org/https://doi.org/10.1016/j.ceramint.2019.10.245.

[13] A. Ghazanfari, W. Li, M.-C. Leu, G. Hilmas, Novel Extrusion-Based Additive Manufacturing Process for Ceramic Parts, in: Solid Free. Fabr. 2016, 2016: pp. 1509–1529.

[14] G.H. Loh, E. Pei, D. Harrison, M.D. Monzon, An overview of functionally graded additive manufacturing, Addit. Manuf. 23 (2018) 34–44.

[15] J.W. Jung, J.-S. Lee, D.-W. Cho, Computer-aided multiple-head 3D printing system for printing of heterogeneous organ/tissue constructs, Sci. Rep. 6 (2016) 21685.

[16] H.-W. Kang, S.J. Lee, I.K. Ko, C. Kengla, J.J. Yoo, A. Atala, A 3D bioprinting system to produce human-scale tissue constructs with structural integrity, Nat. Biotechnol. 34 (2016) 312–319.

[17] J.C.S. McCaw, E. Cuan-Urquizo, Curved-Layered Additive Manufacturing of non-planar, parametric lattice structures, Mater. Des. 160 (2018) 949–963. https://doi.org/https://doi.org/10.1016/j.matdes.2018.10.024.

[18] S. Babu, The future of additive manufacturing is all about design, Eng. (2017). https://www.theengineer.co.uk/the-future-of-additive-manufacturing-is-all-about-design/ (accessed July 17, 2020).

[19] regenHU BioCAD, (2020). https://www.regenhu.com/3d-bioprinters/software.

[20] B. Wong, G-Code Generator, (2020). https://github.com/brendanwong/g-code-generator.

[21] E. Nyberg, A. O'Sullivan, W. Grayson, ScafSlicr: A MATLAB-based slicing algorithm to enable 3D-printing of tissue engineering scaffolds with heterogeneous porous microarchitecture, PLoS One. 14 (2019) e0225007. https://doi.org/10.1371/journal.pone.0225007.

[22] Aura, (2020). https://anisoprint.com/product-aura.

[23] Eiger, (2020). https://markforged.com/eiger/.

[24] Fibrify, (2020). https://www.9tlabs.com/product.

[25] C. Bailey, E. Aguilera, D. Espalin, J. Motta, A. Fernandez, M.A. Perez, C. Dibiasio, D. Pryputniewicz, E. Macdonald, R.B. Wicker, Augmenting Computer-Aided Design Software With Multi-Functional Capabilities to Automate Multi-Process Additive Manufacturing, IEEE Access. 6 (2018) 1985–1994. https://doi.org/10.1109/ACCESS.2017.2781249.

[26] S. Koda, H. Tanaka, Direct G-code manipulation for 3D material weaving, in: Nanosensors, Biosensors, Info-Tech Sensors 3D Syst. 2017, 2017. https://doi.org/10.1117/12.2261648.

[27] G.C. Anzalone, B. Wijnen, J.M. Pearce, Multi-material additive and subtractive prosumer digital fabrication with a free and open-source convertible delta RepRap 3-D printer, Rapid Prototyp. J. 21 (2015) 506–519. https://doi.org/10.1108/RPJ-09-2014-0113.

[28] G. Hodgson, A. Anellucci, J. Moe, Slic3r Manual: Post-Processing Scripts, (2020). https://manual.slic3r.org/advanced/post-processing (accessed July 17, 2020).

[29] S.A. Tronvoll, C.W. Elverum, T. Welo, Dimensional accuracy of threads manufactured by fused deposition modeling, Procedia Manuf. 26 (2018) 763–773.

[30] D.O. Visscher, A. Gleadall, J.K. Buskermolen, F. Burla, J. Segal, G.H. Koenderink, M.N. Helder, P.P.M. van Zuijlen, Design and fabrication of a hybrid alginate hydrogel/poly (ε-caprolactone) mold for auricular cartilage reconstruction, J. Biomed. Mater. Res. Part B Appl. Biomater. (2018).

[31] A. Moetazedian, A.S. Budisuharto, V. V. Silberschmidt, A. Gleadall, CONVEX (CONtinuously Varied EXtrusion): a new scale of design for additive manufacturing, Addit. Manuf. 37 (2021) 101576. https://doi.org/10.1016/j.addma.2020.101576.

[32] M. Littwin, R. Littwin, Repetier Host, (2020). https://www.repetier.com/download-software/.

[33] Desmos graphing calculator, (2021). https://www.desmos.com/calculator.

[34] A. Gleadall, Data for article: FullControl GCode Designer - open-source software for unconstrained design in additive manufacturing, (2021). https://doi.org/doi:10.17028/rd.lboro.12933320.

[35] M. Shomper, Designing Lattice Structures for Biologically-Relevant Medical Implants, (2019). https://ntopology.com/blog/2019/07/25/designing-and-building-lattice-structures-for-biologically-relevant-medical-implants/.

[36] A. Moetazedian, A. Gleadall, X. Han, V.V. Silberschmidt, Effect of environment on mechanical properties of 3D printed polylactide for biomedical applications, J. Mech. Behav. Biomed. Mater. 102 (2020). https://doi.org/https://doi.org/10.1016/j.jmbbm.2019.103510.

[37] J. Allum, A. Moetazedian, A. Gleadall, V. V Silberschmidt, Interlayer bonding has bulk-material strength in extrusion additive manufacturing: new understanding of anisotropy, Addit. Manuf. (2020) 101297. https://doi.org/10.1016/j.addma.2020.101297.

[38] J. Allum, J. Kitzinger, L. Yimeng, V. V. Silberschmidt, A. Gleadall, ZigZagZ: improving mechanical performance in extrusion additive manufacturing by nonplanar toolpaths, Addit. Manuf. 38 (2021) 101715. https://doi.org/10.1016/j.addma.2020.101715.

[39] A. Gleadall, W. Poon, J. Allum, A. Ekinci, X. Han, V. V. Silberschmidt, Interfacial fracture of 3D-printed bioresorbable polymers, Procedia Struct. Integr. 13 (2018) 625–630. https://doi.org/https://doi.org/10.1016/j.prostr.2018.12.103.